行政院國家科學委員會專題研究計劃期中報告

※※※※※※※※※※※※※※※※※※※※※※※※※※※※※※※※※※
※　　　　　　　　　　　　　　　　　　　　　　　　　　　　　　　　※
※ 回流型薄膜萃取器之最佳回流隔板位置及效率之提高(1/3) ※
※　　　　　　　　　　　　　　　　　　　　　　　　　　　　　　　　※
※※※※※※※※※※※※※※※※※※※※※※※※※※※※※※※※※※

計畫類別：■個別型計畫　　　□整合型計畫

計畫編號：NSC 91-2214-E-032-001

執行期間：91 年 8 月 1 日至 92 年 7 月 31 日

個別型計劃：計畫主持人：葉和明
　　　　　　共同主持人：

整合型計劃：總計畫主持人：
　　　　　　子計劃主持人：

註：整合型計劃總報告與子計劃成果報告請分開編印各
　成一冊，彙整一起繳送國科會。

處理方式：□可立即對外提供參考
　　　　　□一年後可對外提供參考
　　　　　■兩年後可對外提供參考
　　　　　　(必要時，本會得展延發表時限)

執行單位：淡江大學化工研究所

中華民國九十二年五月二十五日

回流型薄膜萃取器之最佳回流隔板位置及效率之提高(1/3)

1. Influence of channel-width ratio on solvent extraction through a double-pass parallel-plate membrane module with or without recycle

H. M. Yeh*, C. H. Chen, T. Y. Yueh
Department of Chemical Engineering, Tamkang University, Tamsui, Taiwan 251

Abstract

The effect of the location of a impermeable barrier, which is placed for double pass in the raffinate phase, on solvent extraction through a parallel-plate membrane module with or without recycle, has been investigated. Theoretical predictions are in fairly good agreement with the experimental results. Considerable improvement in performance is obtainable if the subchannel width, as well as the mass-transfer area, of countercurrent flow is as large as possible than that of concurrent flow, especially for the operation of small recycle ratio and low flow rate. It has been also checked that the hydraulic dissipated energy due to the friction loss of fluid flow is very small and thus, the operating cost in all devices may be ignored.

Keyword: Membrane extraction; Double pass; Recycle; Channel-width ratio

*Corresponding author. Tel. : +886-02-9180149; fax: +886-02-26203887
E-mail address: hmyeh@mail.tku.edu.tw (H. M. Yeh)

1. Introduction

Applications of the recycle-effect concept in the design and operation of the equipment with external or internal refluxes can effectively enhance the effect on heat and mass transfer, leading to improved performance [1-11]. Recently, the recycle effect on solvent extraction in microporous-membrane modules has been studied both theoretically and experimentally [12, 13]. For solvent extraction through a membrane modules, the recycle effect is favorable for the system with higher distribution coefficients where the liquid-phase mass-transfer resistances are more extremely predominant. It is the purpose of this work to investigate the influence of width ratio of flow subchannels in the raffinate phase on solvent extraction through a double-pass parallel-plate membrane module with or without recycle.

2. Theory

Membrane extraction is carried out in a microporous membrane device, in which the membrane is generally contacted with two immiscible fluids at two sides (phases *a* and *b*). However, if these two fluids are miscible, then the pores of the membrane is filled with another fluid (phase *c*) which is immiscible with these two fluids. The solute is extracted from phase *a* to phase *c* and then to phase *b*, or vice versa. This new technique overcomes the limitations of conventional liquid extraction, such as flooding, intimate mixing, limitations on independent phases flow rate variations, requirement of density difference and inability to handle particulates [14].

2. *1. Governing equations*

Fig. 1 shows the double-pass parallel-plate membrane extractor with recycle. An impermeable plate with negligible thickness is placed in vertical to the upper plate and the membrane sheet, at a certain line of channel *a* (phase *a*) to divide the channel into two subchannels (subchannels a_1 and a_2) of widths Δw and $(1-\Delta)\, w$, and that a pump is installed for recycle. Thus, in the raffinate phase (phase *a*), the inlet fluid of volume rate Q_a mixed with the recycle outlet fluid of volume rates RQ_a, flows steadily as well as concurrently and countercurrently within subchannels a_1 and a_2, respectively. The extract phase (phase *b*) with inlet volume rate Q_b flows steadily through channel *b*.

Referring to Fig. 1, the mass balance over the right-hand section of the membrane extractor operated, with reflux ratio *R*, is

$$Q_b(C_{b,e} - C_b) = (1+R)Q_a(C_{a,1} - C_{a,2}) \tag{1}$$

or

$$C_b = C_{b,e} - (\frac{Q_a}{Q_b})(1+R)(C_{a,1} - C_{a,2}) \tag{2}$$

Considering the mass transfer on subchannels a_1 and a_2 over the length *dx*

$$-(1+R)Q_a dC_{a,1} = K_1 \Delta w(H_{ac}C_{a,1} - H_{bc}C_b)dx \tag{3}$$

$$(1+R)Q_a dC_{a,2} = K_2(1-\Delta)w(H_{ac}C_{a,2} - H_{bc}C_b)dx \tag{4}$$

where K_1 and K_2 are the overall mass-transfer coefficients in subchannels a_1 and a_2, respectively, while H_{ac} and H_{bc} are the distribution coefficients between two different phases, as defined by

$$H_{ac} = \frac{\text{solute concentration in phase c}}{\text{solute concentration in phase a}} \tag{5}$$

Substituting the value of C_b from Eq. (2) into Eq. (3) and (4) gives

$$\frac{dC_{a,1}}{dx} + \zeta C_{a,1} + \phi C_{a,2} = \xi C_{b,e} \tag{6}$$

$$\frac{dC_{a,2}}{dx} + \omega C_{a,2} + \eta C_{a,1} = \theta C_{b,e} \tag{7}$$

where

$$\zeta = K_1 \Delta w[\frac{H_{ac}}{(1+R)Q_a} + \frac{H_{bc}}{Q_b}] \tag{8}$$

$$\phi = -K_1 \Delta w(\frac{H_{bc}}{Q_b}) \tag{9}$$

$$\xi = \frac{K_1 \Delta w}{(1+R)}(\frac{H_{bc}}{Q_a}) \tag{10}$$

$$\omega = -K_2(1-\Delta)w[\frac{H_{ac}}{(1+R)Q_a} - \frac{H_{bc}}{Q_b}] \tag{11}$$

$$\eta = -K_2(1-\Delta)w(\frac{H_{bc}}{Q_b}) \tag{12}$$

$$\theta = -\frac{K_2(1-\Delta)w}{(1+R)}(\frac{H_{bc}}{Q_a}) \tag{13}$$

2. 2. Concentration distributions

Eqs. (6) and (7) can be solved simultaneously for solute concentrations, $C_{a,1}$ and $C_{a,2}$, in subchannels a_1 and a_2 with the following boundary conditions:

at $x=l$, $C_{a,1} = C_{a,2} = C'_{a,e}$ (14)

The results are

$$C_{a,1} = \alpha e^{\lambda_a x} + \beta e^{\lambda_b x} + fC_{b,e} \tag{15}$$

$$C_{a,2} = \frac{1}{\phi}[-(\lambda_a + \zeta)\alpha e^{\lambda_a x} - (\lambda_b + \zeta)\beta e^{\lambda_b x} + (\xi - \zeta f)C_{b,e}] \tag{16}$$

where

$$\lambda_a = \frac{-(\zeta+\omega)+\sqrt{(\zeta-\omega)^2+4\phi\eta}}{2} \tag{17}$$

$$\lambda_b = \frac{-(\zeta+\omega)-\sqrt{(\zeta-\omega)^2+4\phi\eta}}{2} \tag{18}$$

$$f = \frac{\omega\xi-\phi\theta}{\zeta\omega-\phi\eta} \tag{19}$$

where α and β are the integration constants which are determined by Eq. (14) as

$$\alpha = \frac{e^{-\lambda_a l}}{(\lambda_a-\lambda_b)}[(f\lambda_b+\xi)C_{b,e}-(\lambda_b+\zeta+\phi)C'_{a,e}] \tag{20}$$

$$\beta = \frac{e^{-\lambda_b l}}{(\lambda_a-\lambda_b)}[-(f\lambda_a+\xi)C_{b,e}+(\lambda_a+\zeta+\phi)C'_{a,e}] \tag{21}$$

If mixed inlet concentration $C^o_{a,i}$ and the outlet concentration $C_{a,e}$ are introduced into Eqs. (15) and (16), respectively, i.e.

at $x=0$, $C_{a,1}=C^o_{a,i}$ (22)

at $x=0$, $C_{a,2}=C_{a,e}$ (23)

one obtains, with the substitution of Eqs. (20) and (21)

$$C^{\circ}_{a,i} = AC_{b,e}-BC'_{a,e} \tag{24}$$

$$C_{a,e} = EC_{b,e}-FC'_{a,e} \tag{25}$$

where

$$A = \frac{(f\lambda_b+\xi)e^{-\lambda_a l}-(f\lambda_a+\xi)e^{-\lambda_b l}}{(\lambda_a-\lambda_b)}+f \tag{26}$$

$$B = \frac{(\lambda_b+\zeta+\phi)e^{-\lambda_a l}-(\lambda_a+\zeta+\phi)e^{-\lambda_b l}}{(\lambda_a-\lambda_b)} \tag{27}$$

$$E = \frac{1}{\phi}[\frac{-(\lambda_a + \zeta)(f\lambda_b + \xi)e^{-\lambda_a l} + (\lambda_b + \zeta)(f\lambda_a + \xi)e^{-\lambda_b l}}{(\lambda_a - \lambda_b)} + (\xi - \zeta\ f)] \tag{28}$$

$$F = \frac{1}{\phi}[\frac{-(\lambda_a + \zeta)(\lambda_b + \zeta + \phi)e^{-\lambda_a l} + (\lambda_b + \zeta)(\lambda_a + \zeta + \phi)e^{-\lambda_b l}}{(\lambda_a - \lambda_b)}] \tag{29}$$

Inspection of Eqs. (24) and (25) shows that the outlet concentrations, $C'_{a,e}$, $C_{a,e}$ and $C_{b,e}$, as well as the mixed inlet concentration $C^{o}_{a,i}$, are not specified a priori. Mathematically, two more relations are needed for determination of these values. For this purpose, two mass balances for solutes at the inlet of phase *a* and through the whole module are readily obtained, respectively, as

$$C_{a,i} + RC_{a,e} = (1+R)C^{\circ}_{a,i} \tag{30}$$

$$C_{b,e} = C_{b,i} + (\frac{Q_a}{Q_b})(C_{a,i} - C_{a,e}) \tag{31}$$

Solving Eqs. (24), (25), (30) and (31), simultaneously, one has the outlet solute concentrations as

$$C_{a,e} = \frac{[FQ_b - (1+R)(AF - BE)Q_a]C_{a,i} - [(1+R)(AF - BE)Q_b]C_{b,i}}{[(1+R)B - FR]Q_b - (1+R)(AF - BE)Q_a} \tag{32}$$

$$C_{b,e} = \frac{\left[\frac{F}{(1+R)B - FR}\right]C_{a,i} - C_{a,e}}{\left[\frac{(1+R)(AF - BE)}{(1+R)B - FR}\right]} \tag{33}$$

2. 3. Mass-transfer rate

Once $C_{a,e}$(or $C_{b,e}$) is calculated from Eq. (32) [or Eq. (33)], the total

mass-transfer rate will be determined by Eq. (34), modified from Eq. (31)

$$W = Q_a(C_{a,i} - C_{a,e}) = Q_b(C_{b,e} - C_{b,i}) \tag{34}$$

3. Experiments

The chemicals, materials, dimensions of apparatus and experimental procedure are exactly the same as those employed and performed in previous work [12], except that in present experimental work, the impermeable plate of negligible thickness, instead of being placed at the center line of channel *a*, was placed at arbitrary location and in vertical to the upper plate and the membrane sheet to divide channel *a* into two subchannels (subchannels a_1, and a_2) of height h and variable widths (i.e., Δ=0.25, 0.5 and 0.75), as shown in Fig.1.

Experiments were carried out with the use of a membrane sheet (l=w=0.165m) made of microporous polypropylene(Gelman Sciences, average pore size=0.2 μm, porosity=70% and thickness=178 μm) as a permeable barrier to extract acetic acid(reagent ACS grade, Fisher) from aqueous solution by methyl isobutyl ketone (MIBK, regent grade, Fisher). The membrane sheet was inserted in parallel between two parallel plates of stainless steel, with same distance from them to divide the conduit into two channels(channels *a* and *b*, or phases *a* and *b*) of same height ($h = 1.9 \times 10^{-3}$ m). Since microporous polypropylene is hydropholic membranes, the organic solution (solute: acetic; solvent: MIBK) wets the membrane, and thus $H_{bc} = H_{bb} = 1$ and $H_{ac} = H_{ab} = 0.524$ at $25\,^{o}C$ [16].

4. Results and discussion

4.1. Comparison of theoretical predictions with experimental results

Many experimental data of various operating conditions for outlet solute concentration in phase *a*, $C_{a,e}$, were obtained [17] and the corresponding values of mass-transfer rate, *W*, were then calculated from Eq. (34). Some of the experimental results are plotted in Fig.2.

It was found in previous work [12] that all overall mass-transfer coefficients vary linearly with Q_a, as well as with the fluid velocities, $v_{a,1}$ and $v_{a,2}$, in such small velocity range performed in present study, while over a lager range of velocities the mass transfer coefficients actually vary with velocity to the one-third power [18]. The following correlation equations for K_1 (cocurrent flow) and K_2 (countercurrent flow) in terms of $v_{a,1}$ and $v_{a,2}$, respectively, were reached [12], applicable to the range of experimental conditions.

For $C_{a,i} = 5\times10^{-4} mole/cm^3$:

$$K_1 \times 10^4 (cm/s) = 3.865 + 1.484 v_{a,1} (cm/s) \tag{35}$$

$$K_2 \times 10^4 (cm/s) = 5.016 + 0.718 v_{a,2} (cm/s) \tag{36}$$

For $C_{a,i} = 2.02\times10^{-3}$ $mole/cm^3$:

$$K_1 \times 10^4 (cm/s) = 2.152 + 0.846 v_{a,1} (cm/s) \tag{37}$$

$$K_2 \times 10^4 (cm/s) = 3.177 + 0.733 v_{a,2} (cm/s) \tag{38}$$

In Eqs. (35)-(38)

$$v_{a,1} = \frac{Q_a(1+R)}{h\Delta w} \tag{39}$$

$$v_{a,2} = \frac{Q_a(1+R)}{h(1-\Delta)w} \tag{40}$$

The theoretical predictions of mass-transfer rate were calculated from Eqs. (32) and (34) with the use of Eqs. (35)-(38), and some of them are also plotted in Fig. 2 for comparison. It is seen in these figures that the theoretical predictions are qualitative agreement with the experimental results, and that W increase with R and Q_a, as well as with the decrease of subchannel-width ratio Δ.

4.2. Effect of Δ on mass-transfer rate

It is seen in Fig.2 that the mass-transfer rate increases as the width of subchannel a_1, Δw, decreases (or the width of subchannel a_2 increases). This is because that for mass transfer, the countercurrent flow in subchannel a_2 is more effective than the cocurrent flow in subchannel a_1, and that larger mass-transfer area for countercurrent-flow channel is beneficial to total mass-transfer rate.

Fig.3 shows the comparison of mass-transfer rate W obtained in the devices of R=0(without recycle) and Δ=0.1~0.5 with that in the devices of Δ=0.5 (with the impermeable plate placed at the center line of raffinate phase) and R=1~7. It is seen in this figure that for lower flow rate, Q_a, the modules of small Δ without recycle overcomes the modules of Δ=0.5 with recycle. As we can see that under lower flow-rate operation, the value of W for Δ=0.1 and R=0 is lager than that for Δ=0.5 and $R \le 7$, say $Q_a < 0.2\, cm^3/s$, and even lager than the mass-transfer rate for Δ=0.5 and

R=1 under higher flow-rate operation, say Q_a<0.9 cm^3/s.

Fig.4 illustrates the comparison of mass-transfer rate obtained in the devices of R=1 and Δ=0.1~0.5 with that in the devices of Δ=0.5 and R=2~7. The results are similar to that in Fig.3. It is concluded that under lower flow-rate operation, the performance of a device of R=0 with Δ decreasing overcomes a device of Δ=0.5 with R increasing. In other words, instead of setting the recycle operation with large recycle ratio and Δ=0.5, the mass-transfer rate for membrane extraction in a double-pass parallel-plate module can be also improved by adjusting the place of the impermeable barrier away from the center line (Δ=0.5) of the raffinate phase to arrange the width, $(1-\Delta)w$, of countercurrent-flow subchannel as large as possible than that, Δw, of concurrent-flow subchannal if the operation is carried out at low flow rate.

Some numerical values of predicting result for W are listed in Tables 1 and 2, which give the same conclusion described above.

4.3. Effect of Δ on hydraulic dissipated energy

In present study, an impermeable barrier with negligible thickness is placed in vertical to the upper plate and membrane sheet, at an adjustable location of channel a (phase a) to divide the channel into two subchannels (subchannels a_1 and a_2) of widths Δw and $(1-\Delta)w$ for double pass as well as for recycle. Though considerable improvement in mass transfer can be obtained by adjusting the location of barrier plate, and/or operating with recycle, the hydraulic dissipated energy due to the friction loss of fluid flow should be discussed.

The hydraulic dissipated power in a parallel-plate channel may be estimated by

$$E = (\textit{fluid density} \times \textit{volumn flow rate}) \times \frac{\Delta P}{\textit{fluid density}}$$

$$= (\textit{volume flow rate}) \times \Delta P \tag{41}$$

If laminar flow in the flow channels is assumed, the pressure drop through the flow channel is [15]

$$\Delta P = \frac{12\mu\, l \times (\textit{volumn flow rate})}{h^2 \times (\textit{cross} - \textit{section area of channel})} \tag{42}$$

Since the total hydraulic dissipated energy includes those in subchannel a_1, subchannel a_2 and channel b, we have

$$E = E_{a,1} + E_{a,2} + E_b$$

$$= \left[Q_a(1+R) \times \frac{12\mu_a l\ Q_a(1+R)}{h^3 \Delta w} \right] + \left[Q_a(1+R) \times \frac{12\mu_a l\ Q_a(1+R)}{h^3 (1-\Delta) w} \right] + \left[Q_b \times \frac{12\mu_b l\ Q_b}{h^3 w} \right]$$

$$= \frac{12l}{h^3 w} \left[\frac{\mu_a {Q_a}^2 (1+R)^2}{\Delta(1-\Delta)} + \mu_b {Q_b}^2 \right] \tag{43}$$

The total hydraulic dissipated energies E for various operating conditions were calculated by Eq. (43) with l=w=16.5cm, h=0.19cm, $\mu_a = 1\times10^{-2}\, g/cm\cdot s$ and $\mu_b = 0.58\times10^{-2}\, g/cm\cdot s$. Some of the results of E are also listed in Tables 1 and 2. It is shown in these tables that E increases when Δ goes far from 1/2 as well as R and/or Q_a increases. However the hydraulic dissipated energy is very small even for the system of extremely small Δ (or 1-Δ) and large R and Q_a where E is the largest. For instance, $E = 2.21\times10^{-6}\, hp$ for Δ =0.1 (or 0.9), R=9 and

Q_a=1.309 cm^3/s. Therefore, operating cost in all devices may be ignored.

5. Conclusion

The predicting equations for mass-transfer rate in double-pass parallel-plate membrane extractors of arbitrary barrier location with or without recycle, has been derived by mass balances. Experimental works were carried out in a parallel conduit of stainless steel inserted with a membrane sheet made of microporous polypropylene to extract acetic acid from aqueous solution (phase *a*) by methyl iso-butyl ketone. Since the organic solution (phase *b*) wetted the membrane during operation, the membrane used in this study is hydrophobic. Theoretical predictions are qualitative agreement with the experimental results.

Instead of setting the recycle operation with large recycle ratio and Δ=0.5, considerable improvement in mass transfer can be also achieved for low flow rate operation if the location of impermeable barrier for double pass is away from the center line (Δ=0.5) with Δ (or 1-Δ) as small as possible, say Δ=0.1. Since the hydraulic dissipated energies are extremely small even operating with recycle or with the change of the barrier location as shown in Tables1 and 2, the operating cost in all devices may be ignored.

6. List of symbols

A, *B*, *E*, *F*	Constant defined by Eqs. (26)-(29).
C_a, C_b	Bulk solute concentrations in phase *a*. and in phase *b* ($mole/cm^3$)

$C_{a,e}, C_{b,e}$	Outlet solute concentrations in phase *a*. and in phase *b* ($mole/cm^3$)
$C'_{a,e}$	Outlet concentrations in subchannel a_1, or inlet concentration in subchannel a_2 ($mole/cm^3$)
$C_{a,i}, C_{b,i}$	Inlet solute concentrations in phase *a*. and in phase *b* ($mole/cm^3$)
$C^o_{a,i}$	Mixed inlet concentration in phase *a* ($mole/cm^3$)
C_{a1}, C_{a2}	Bulk solute concentrations in subchannel a_1, in subchannel a_2 of phase a ($mole/cm^3$)
E	Hdraulic dissipated power (hp)
f	Constant defined by Eq. (19)
H_{ij}	Distribution coefficient between phase *i* and phase *j*
h	Half height of parallel channel, or distance between flat plate and membrane sheet (cm)
K	Average overall mass-transfer coefficient (cm/s)
K_1, K_2	K for concurrent, and for countercurrent flow (cm/s)
l	The length of membrane sheet (cm)
ΔP	Pressure drop in flow channel (N/cm^2)
Q_a, Q_b	Inlet volume rates in phase *a*, and in phase *b* (cm^3/s)
R	Reflux ratio, reverse volume rate RQ_a divided by inlet volume rate Q_a
S	Overall mass-transfer area of a flat-plate membrane module lw, (cm^2)
$v_{a,1}, v_{a,2}$	Fluid velocity in subchannel a_1, in subchannel a_2 (cm/s)

v_b	Fluid velocity in phase b (cm/s)
w	Width of membrane sheet (cm)
x	Axis along the flow direction

6. 1. Greek letters

α	Constant defined by Eq. (20)
β	Constant defined by Eq. (21)
Δ	Width ratio of subchannel a_1 to subchannel a_2
ζ,ϕ,ξ	Constant defined by Eqs. (8), (9) and (10), respectively
ω,η,θ	Constant defined by Eqs. (11), (12) and (13), respectively
λ_a,λ_b	Constant defined by Eqs. (17) and (18), respectively
ε	Porosity of membrane
τ	Pore tortuosity of membrane
μ_a,μ_b	Fluid viscosities of phase a and b, respectively ($g/cm\cdot s$)

7. Acknowledgements

We wish to express our thanks to the National Science Council of R. O. C. for financial aid under Grand No. NSC-91-2214-E-032-001.

8. References

[1] S.W. Tsai, H.M. Yeh, A study of the separation efficiency in horizontal thermal diffusion columns with external refluxes, Can. J.

Chem. Eng. 63 (1985) 406.

[2] H.M. Yeh, S.W. Tsai, C.S. Lin, A study of the separation efficiency in thermal diffusion column with a vertical permeable barrier, AIChE J. 32 (1986) 971.

[3] H.M. Yeh, T.W. Cheng, S.W. Tsai, A study of the gratez problem in concentric-tube continuous-contact countercurrent separation processes with recycles at both ends, Sep. Sci. Technol. 21 (1986) 403.

[4] H.M. Yeh, S.W. Tsai, C.L. Chiang, Recycle effects on heat and mass transfer through a parallel-plate channel, AIChE J. 33 (1987) 1743.

[5] C.D. Ho, H.M. Yeh, W.S. Sheu, The analytical studies of heat and mass transfer through a parallel-plate channel with recycle, Int. J. Heat Mass Transfer 41 (1988) 2589.

[6] J. Korpijarvi, P. Oinas, J. Reunanen, Hydrodynamics and mass transfer in airlift reactor, Chem. Eng. Sci. 54 (1998) 2255.

[7] E. Santacesaria, M. Di Serio, P. Iengo, Mass transfer and kinetics in ethoxylation spray tower loop reactors, Chem. Eng. Sci. 54 (1999) 1499.

[8] E. Garcia-Calvo, A. Rodriguez, A. Prados, J. Klein, Fluid dynamic model for three-phase airlift reactors, Chem. Eng. Sci. 54 (1998) 2359.

[9] M. Stenas, M. Clark, V. Lazarova, Holdup and liquid circulation velocity in a rectangular air-lift bioreactor, Ind. Eng. Chem. Res. 38 (1999) 944.

[10] S. Goto, P.D. Gaspillo, Effect of static mixer on mass transfer in draft

tube bubble column and in external loop cilomn, Chem. Eng. Sci. 47 (1992) 3533.

[11] K.I. Kikuchi, H. Takahashi, Y. Takeda, F. Sugawara, Hydrodynamic behavior of single particles in a draft-tube bubble column, Can. J. Chem. Eng. 77 (1999) 573.

[12] H.M. Yeh, Y.Y. Peng, Y.K. Chen, Solvent extraction through a double-pass parallel-plate membrane channel with recycle, J. Membr. Sci. 163 (1999) 177.

[13] H.M. Yeh, C.H. Chen, Recycle effects on solvent extraction through concurrent-flow parallel-plate membrane modules, J. Membr. Sci. 190(2001) 35.

[14] T.C. Lo, M.H.I. Baird, Liquid-Liquid extraction, in: M. Grayson (Ed.), Kirktothmer Encyclopedia of Chemical Technology, Vol. 9, 3rd Edition, Wiley, New York, 1980.

[15] R.B. Bird, W.E. Stewart, E.N. Lightfoot, Transport Phenomena, Wiley, Inc., New York, 1971, p.62.

[16] H.M. Yeh, C.M. Huang, Solvent extraction in multipass parallel-flow mass exchangers of microporous hollow-fiber modules, J. Membr. Sci. 103 (1995) 135.

[17] C.H. Chen, The effect of various-type recycles on concurrent-flow solvent extraction in flat-plat membrane module, MS thesis, Tamkang University, Tamsui, Taiwan 251, ROC, 2001.

[18] M.C. Poter, handbook of Industrial Membrane Technology, Noyes Publications, New Jersey, 1990, pp.1-3, p.175.

Figure Legends

Fig.1. Schematic diagram of double-pass parallel-plate membrane extractors with Recycle.

Fig.2. Comparison of theoretical predictions with experimental results, $Q_a = 0.442 cm^3/s$, $Q_b = 0.25 cm^3/s$.

Fig.3. Comparison of W obtained in the devices of R=0 and Δ=0.1~0.5 with that in the devices of Δ=0.5 and R=1~7.

Fig.4. Comparison of W obtained in the devices of R=1 and Δ=0.1~0.5 with that in the devices of Δ=0.5 and R=2~7.

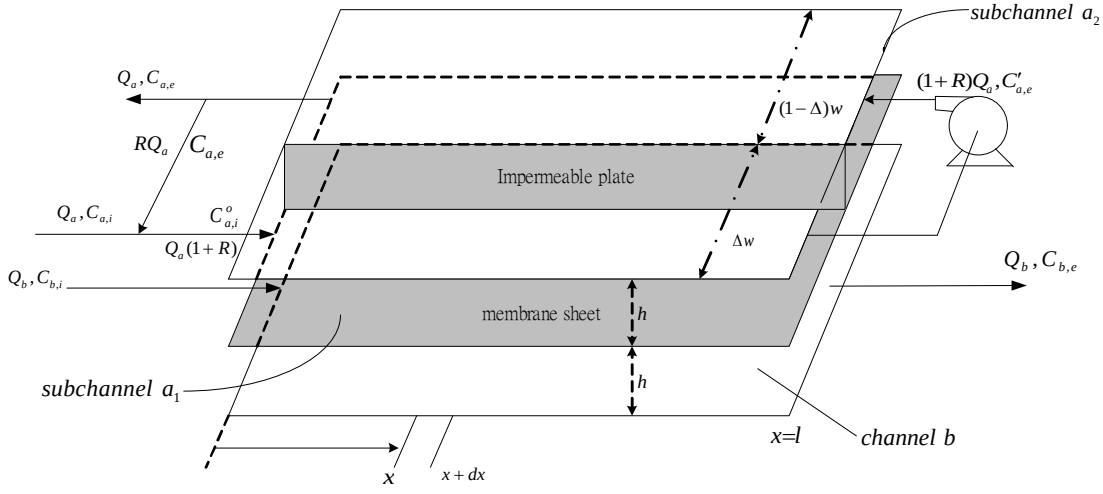
subchannel a_2
$Q_a, C_{a,e}$
$(1+R)Q_a, C'_{a,e}$
$(1-\Delta)w$
RQ_a
$C_{a,e}$
Impermeable plate
$Q_a, C_{a,i}$
$C^o_{a,i}$
$Q_a(1+R)$
Δw
$Q_b, C_{b,i}$
$Q_b, C_{b,e}$
membrane sheet
h
h
subchannel a_1
$x=l$
channel b
x
$x+dx$

Fig. 1.

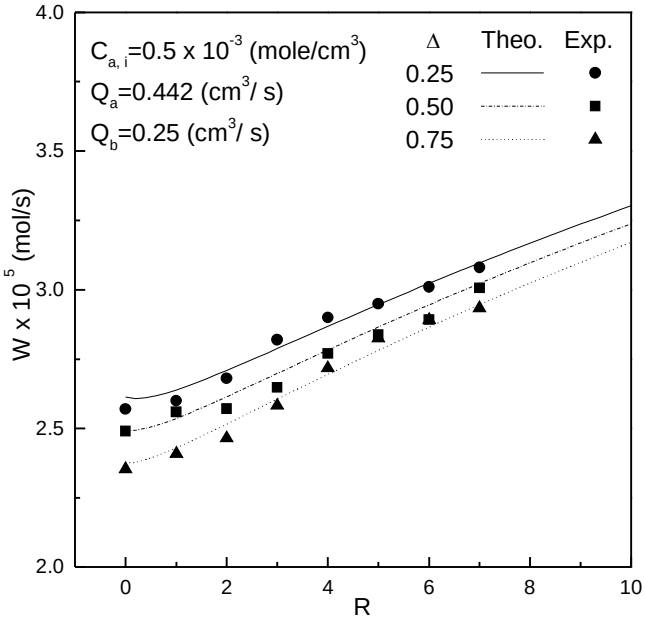

(a) $C_{a,i} = 0.5 \times 10^{-3} mole/cm^3$

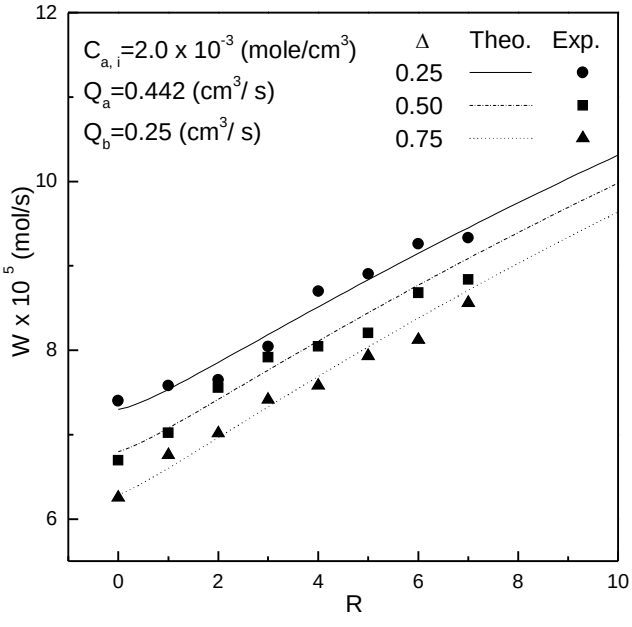

(b) $C_{a,i} = 2.0 \times 10^{-3} mole/cm^3$

Fig. 2

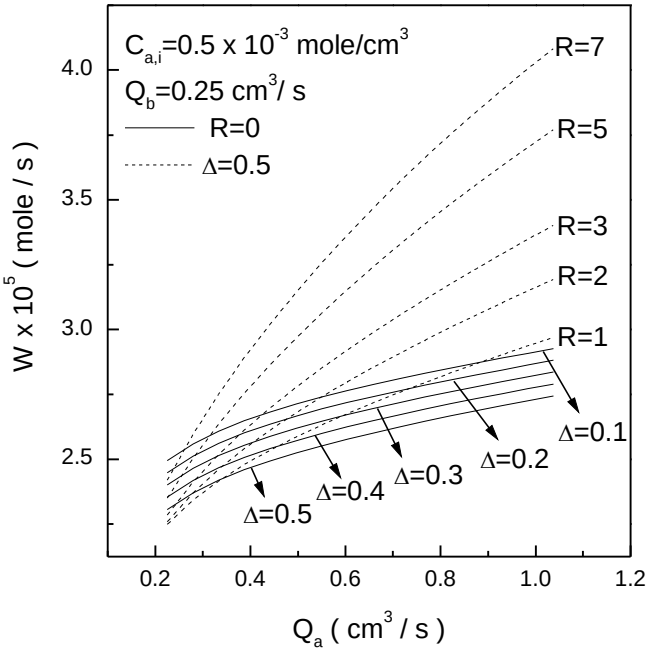

(a) $C_{a,i} = 0.5 \times 10^{-3} mole / cm^3$

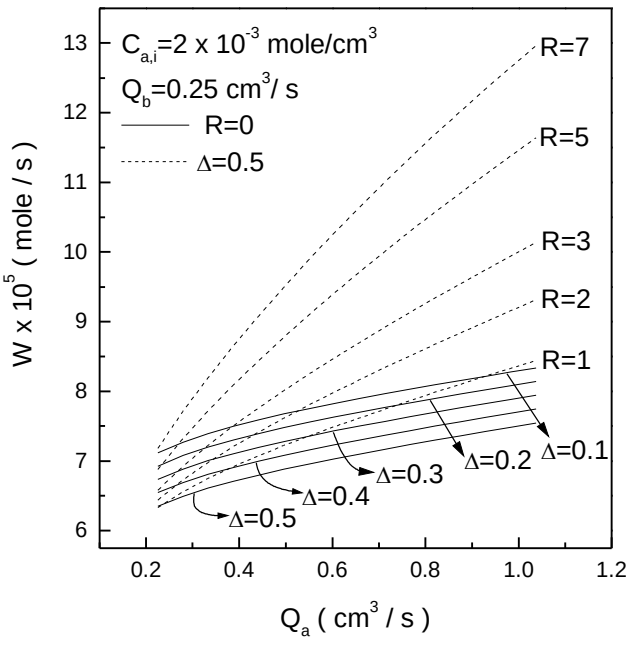

(b) $C_{a,i} = 2.0 \times 10^{-3} mole / cm^3$

Fig. 3

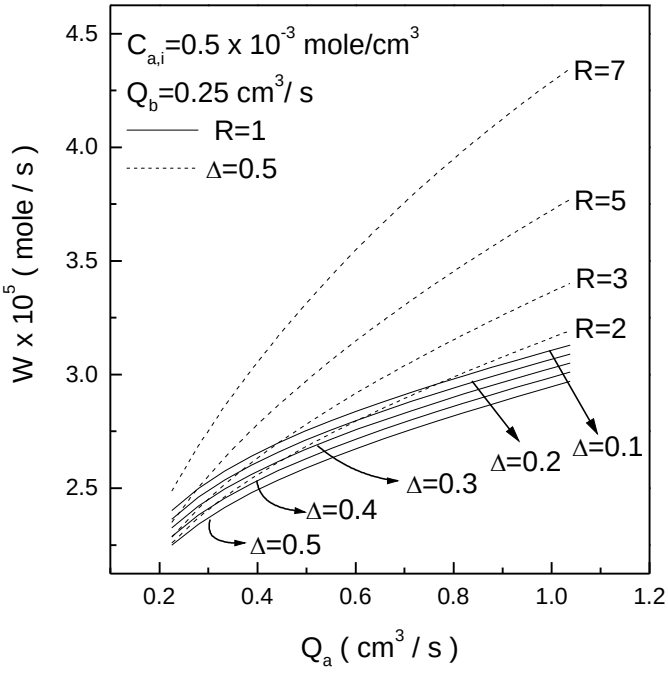

(a) $C_{a,i} = 0.5 \times 10^{-3} mole / cm^3$

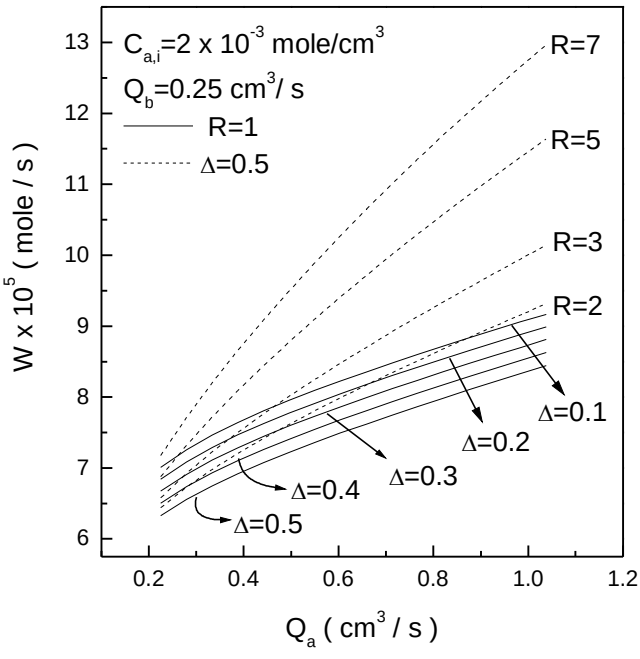

(b) $C_{a,i} = 2.0 \times 10^{-3} mole / cm^3$

Fig. 4

Table 1

Predicting results with $C_{a,i} = 0.5 \times 10^{-3} mole/cm^3$, $Q_b = 0.25 cm^3/s$ and $C_{b,i} = 0$

Q_a (cm^3/s)	R	$W \times 10^5$ (mole/s)				$H \times 10^9$ (hp)		
		$\Delta = 0.1$	$\Delta = 0.25$	$\Delta = 0.5$	$\Delta = 0.75$	$\Delta = 0.1$ or 0.9	$\Delta = 0.25$ or 0.75	$\Delta = 0.5$
0.1	0	2.163	2.098	1.992	1.887	0.14	0.07	0.06
0.1	1	1.972	1.926	1.850	1.772	0.53	0.26	0.20
0.1	5	1.892	1.859	1.802	1.742	4.66	2.24	1.68
0.1	9	1.911	1.882	1.831	1.777	12.92	6.21	4.66
0.2	0	2.456	2.386	2.270	2.153	0.53	0.26	0.20
0.2	1	2.345	2.290	2.197	2.101	2.08	1.00	0.76
0.2	5	2.386	2.343	2.269	2.192	18.60	8.93	6.70
0.2	9	2.488	2.450	2.385	2.316	51.64	24.80	18.60
0.4	0	2.657	2.587	2.468	2.348	2.08	1.00	0.76
0.4	1	2.655	2.595	2.493	2.388	8.27	3.98	2.99
0.4	5	2.910	2.862	2.781	2.697	74.35	35.70	26.77
0.4	9	3.164	3.124	3.056	2.985	206.52	99.13	74.35
0.8	0	2.844	2.775	2.659	2.540	8.27	3.98	2.99
0.8	1	2.981	2.921	2.818	2.713	33.05	15.87	11.91
0.8	5	3.573	3.529	3.454	3.377	297.38	142.75	107.06
0.8	9	4.039	4.006	3.949	3.891	826.03	396.50	297.38

Table 2

Predicting results with $C_{a,i} = 2.0 \times 10^{-3} mole/cm^3$, $Q_b = 0.25 cm^3/s$ and $C_{b,i} = 0$

Q_a (cm^3/s)	R	$W \times 10^5$ (mole/s)				$H \times 10^9$ (kJ/s)		
		$\Delta = 0.1$	$\Delta = 0.25$	$\Delta = 0.5$	$\Delta = 0.75$	$\Delta = 0.1$ or 0.9	$\Delta = 0.25$ or 0.75	$\Delta = 0.5$
0.1	0	6.378	6.129	5.706	5.272	0.14	0.07	0.06
0.1	1	5.976	5.772	5.421	5.053	0.53	0.26	0.20
0.1	5	5.898	5.729	5.433	5.119	4.66	2.24	1.68
0.1	9	6.040	5.883	5.609	5.318	12.92	6.21	4.66
0.2	0	7.026	6.746	6.271	5.784	0.53	0.26	0.20
0.2	1	6.874	6.628	6.207	5.770	2.08	1.00	0.76
0.2	5	7.228	7.017	6.652	6.271	18.60	8.93	6.70
0.2	9	7.693	7.500	7.167	6.818	51.64	24.80	18.60
0.4	0	7.520	7.227	6.729	6.218	2.08	1.00	0.76
0.4	1	7.681	7.414	6.956	6.484	8.27	3.98	2.99
0.4	5	8.791	8.563	8.173	7.768	74.35	35.70	26.77
0.4	9	9.850	9.649	9.305	8.949	206.52	99.13	74.35
0.8	0	8.069	7.774	7.273	6.758	8.27	3.98	2.99
0.8	1	8.673	8.402	7.940	7.464	33.05	15.87	11.91
0.8	5	11.053	10.838	10.469	10.089	297.38	142.75	107.06
0.8	9	13.027	12.851	12.551	12.242	826.03	396.50	297.38

2. Effect of Recycle-Barrier Location on Membrane Extraction in a Parallel-Flow Rectangular Module with Reflux

H. M. Yeh*, F. C. Hung, C. H. Chen, C. R. Hung
Department of Chemical Engineering, Tamkang University, Tamsui, Taiwan 251

Abstract

The influence of recycle-barrier location on membrane extraction through a parallel-flow rectangular module with internal reflux has been investigated. The recycle barrier is placed in the raffinate phase to divide the flow channel into an operating subchannel and a reflux subchannel and thus, there are concurrent flow in one subchannel and countercurrent flow in another subchannel. It was found that larger part of mass-transfer area for countercurrent-flow channel, as well as smaller part of mass-transfer area for concurrent-flow channel, is beneficial to total mass-transfer rate. It was also noted that with the recycle-barrier location moving gradually from the centerline of the raffinate phase to create larger mass-transfer area for countercurrent-flow channel, as well as to decrease mass-transfer area for concurrent-flow channel, the same performance can be achieved with reducing the reflux ratio.

Keyword: Membrane extraction; Reflux; Recycle-barrier location; Parallel flow

*Corresponding author. Tel. : +886-02-9180149; fax: +886-02-26203887
E-mail address: hmyeh@mail.tku.edu.tw (H. M. Yeh)

3. Introduction

Membrane extraction is carried out in a microporous membrane device, in which the membrane is generally contacted with two immiscible fluids at two sides (phases *a* and *b*). However, if these two fluids are miscible, then the pores of the membrane is filled with another fluid (phase *c*) which is immiscible with these two fluids. The solute is extracted from phase *a* to phase *c* and then to phase *b*, or vice versa. This new technique overcomes the limitations of conventional liquid extraction, such as flooding, intimate mixing, limitations on independent phases flow rate variations, requirement of density difference and inability to handle particulates [1].

Application of the external or internal reflux to the design and operation of a mass- or hear- transfer equipment can effectively enhance the effect on mass or heat transfer, leading to improved performance [2-12]. Recently, the recycle effect on solvent extraction in microporous-membrane modules has been studied both theoretically and experimentally [13, 14]. For solvent extraction through a membrane modules, the recycle effect is favorable for the system with higher distribution coefficients where the liquid-phase mass-transfer resistances are more extremely predominant. It is the purpose of this work to investigate the influence of recycle-barrier location in the raffinate phase on solvent extraction through a double-pass parallel-plate membrane module with internal reflux.

4. Theory

Being a parallel-flow device, there are two different flow patterns for operation. Fig. 1 shows the system with concurrent flow first and then followed by

countercurrent flow. On the other hand, Fig. 2 illustrates the system with countercurrent flow first and then followed by concurrent flow.

甲、 *Concurrent-flow operation with countercurrent-flow reflux*

Fig. 1 shows a councurrent-flow rectangular membrane extractor with internal reflux by conuntercurrent flow. An impermeable plate with negligible thickness is placed in vertical to the upper plate and the membrane sheet, at a certain line of channel *a* (phase *a*) to divide the raffinate phase into two subchannels (subchannels a_1 and a_2) of widths Δw and $(1-\Delta)\ w$, respectively, and that a pump is installed for internal reflux. Thus, in the raffinate phase (phase *a*), the inlet fluid of volume rate Q_a mixed with the outlet reflux fluid of volume rate RQ_a, flows steadily as well as concurrently and countercurrently within subchannels a_1 and a_2, respectively. The extract phase (phase *b*) with inlet volume rate Q_b flows steadily through channel *b*.

Referring to Fig. 1, the mass balance over the right-hand section of the membrane extractor operated, with reflux ratio *R*, is

$$Q_b(C_{b,e}-C_b)=(1+R)Q_aC_{a,1}-RQ_aC_{a,2}-Q_aC_{a,e} \tag{1}$$

or

$$C_b=C_{b,e}-(\frac{Q_a}{Q_b})[(1+R)C_{a,1}-RC_{a,2}-C_{a,e}] \tag{2}$$

Considering the mass transfer on subchannels a_1 and a_2 over the length *dx*

$$-(1+R)Q_a dC_{a,1}=K_1\Delta w(H_{ac}C_{a,1}-H_{bc}C_b)dx \tag{3}$$

$$RQ_a dC_{a,2}=K_2(1-\Delta)w(H_{ac}C_{a,2}-H_{bc}C_b)dx \tag{4}$$

where K_1 and K_2 are the overall mass-transfer coefficients in subchannels a_1 and a_2, respectively, while H_{ac} and H_{bc} are the distribution coefficients between two different phases, as defined by

$$H_{ac} = \frac{\text{solute concentration in phase c}}{\text{solute concentration in phase a}} \tag{5}$$

Substituting the value of C_b from Eq. (2) into Eqs. (3) and (4), one obtains

$$\frac{dC_{a,1}}{dx} + \zeta\, C_{a,1} + \zeta^{\circ} C_{a,2} = \varsigma C_{b,e} + \varsigma^{\circ} C_{a,e} \tag{6}$$

$$\frac{dC_{a,2}}{dx} + \varpi\, C_{a,2} + \varpi^{\circ} C_{a,1} = \xi C_{b,e} + \xi^{\circ} C_{a,e} \tag{7}$$

where

$$\zeta = K_1 \Delta w[\frac{H_{ac}}{(1+R)Q_a} + \frac{H_{bc}}{Q_b}] \tag{8}$$

$$\zeta^{\circ} = -\frac{K_1 \Delta w R}{(1+R)}(\frac{H_{bc}}{Q_b}) \tag{9}$$

$$\varsigma = \frac{K_1 \Delta w}{(1+R)}(\frac{H_{bc}}{Q_a}) \tag{10}$$

$$\varsigma^{\circ} = \frac{K_1 \Delta w}{(1+R)}(\frac{H_{bc}}{Q_b}) \tag{11}$$

$$\varpi = -K_2(1-\Delta)w(\frac{H_{ac}}{RQ_a} - \frac{H_{bc}}{Q_b}) \tag{12}$$

$$\varpi^{\circ} = -\frac{K_2(1-\Delta)w(1+R)}{R}(\frac{H_{bc}}{Q_b}) \tag{13}$$

$$\xi = -\frac{K_2(1-\Delta)w}{R}\left(\frac{H_{bc}}{Q_a}\right) \tag{14}$$

$$\xi^{\circ} = -\frac{K_2(1-\Delta)w}{R}\left(\frac{H_{bc}}{Q_b}\right) \tag{15}$$

Eqs. (6) and (7) can be solved simultaneously for solute concentrations, $C_{a,1}$ and $C_{a,2}$, in subchannels a_1 and a_2 with the following boundary conditions:

at $x=L$, $\quad C_{a,1} = C_{a,2} = C_{a,e}$ (16)

The results are

$$C_{a,1} = \alpha e^{\lambda_a x} + \beta e^{\lambda_b x} + nC_{b,e} + mC_{a,e} \tag{17}$$

$$C_{a,2} = \frac{1}{\zeta^0}[-(\lambda_a + \zeta)\alpha e^{\lambda_a x} - (\lambda_b + \zeta)\beta e^{\lambda_b x} + (\varsigma - \zeta n)C_{b,e} + (\varsigma^0 - \zeta m)C_{a,e}] \tag{18}$$

where

$$\lambda_a = \frac{-(\zeta + \varpi) + \sqrt{(\zeta - \varpi)^2 + 4\zeta^{\circ}\varpi^{\circ}}}{2} \tag{19}$$

$$\lambda_b = \frac{-(\zeta + \varpi) - \sqrt{(\zeta - \varpi)^2 + 4\zeta^{\circ}\varpi^{\circ}}}{2} \tag{20}$$

$$n = \frac{\varpi\varsigma - \zeta^{\circ}\xi}{\zeta\varpi - \zeta^{\circ}\varpi^{\circ}} \tag{21}$$

$$m = \frac{\varpi\varsigma^{\circ} - \zeta^{\circ}\xi^{\circ}}{\zeta\varpi - \zeta^{\circ}\varpi^{\circ}} \tag{22}$$

and where α and β are the integration constants which are determined by Eq. (16) as

$$\alpha = \frac{e^{-\lambda_a L}}{(\lambda_a - \lambda_b)}[(n\lambda_b + \varsigma)C_{b,e} + (m\lambda_b + \varsigma^0 - \lambda_b - \zeta - \zeta^0)C_{a,e}] \tag{23}$$

$$\beta = \frac{e^{-\lambda_b L}}{(\lambda_a - \lambda_b)}[-(n\lambda_a + \varsigma)C_{b,e} - (m\lambda_a + \varsigma^0 - \lambda_a - \zeta - \zeta^0)C_{a,e}] \tag{24}$$

If mixed inlet concentration $C^o_{a,i}$ and the outlet reflux concentration $C'_{a,e}$ are introduced into Eqs. (17) and (18), respectively, i.e.

at $x = 0$, $C_{a,1} = C^o_{a,i}$ (25)

at $x = 0$, $C_{a,2} = C'_{a,e}$ (26)

one obtains, with the substitution of Eqs. (23) and (24)

$$C^\circ_{a,i} = AC_{b,e} + BC_{a,e} \tag{27}$$

$$C'_{a,e} = EC_{b,e} + FC_{a,e} \tag{28}$$

where

$$A = \frac{(n\lambda_b + \varsigma)e^{-\lambda_a L} - (n\lambda_a + \varsigma)e^{-\lambda_b L}}{(\lambda_a - \lambda_b)} + n \tag{29}$$

$$B = \frac{(m\lambda_b + \varsigma^\circ - \lambda_b - \zeta - \zeta^\circ)e^{-\lambda_a L}}{(\lambda_a - \lambda_b)}$$

$$- \frac{(m\lambda_a + \varsigma^\circ - \lambda_a - \zeta - \zeta^\circ)e^{-\lambda_b L}}{(\lambda_a - \lambda_b)} + m \tag{30}$$

$$E = \frac{1}{\zeta^\circ}[\frac{(\lambda_a + \zeta)(n\lambda_b + \varsigma)e^{-\lambda_a L}}{(\lambda_b - \lambda_a)}$$

$$- \frac{(\lambda_b + \zeta)(n\lambda_a + \varsigma)e^{-\lambda_b L}}{(\lambda_b - \lambda_a)} + (\varsigma - \zeta n)] \tag{31}$$

$$F = \frac{1}{\zeta^\circ}[\frac{(\lambda_a + \zeta)(m\lambda_b + \varsigma^\circ - \lambda_b - \zeta - \zeta^\circ)e^{-\lambda_a L}}{(\lambda_b - \lambda_a)}$$

$$- \frac{(\lambda_b + \zeta)(m\lambda_a + \varsigma^\circ - \lambda_a - \zeta - \zeta^\circ)e^{-\lambda_b L}}{(\lambda_b - \lambda_a)} + (\varsigma^\circ - \zeta m)] \tag{32}$$

Inspection of Eqs. (27) and (28) shows that the outlet concentrations, $C'_{a,e}$, $C_{a,e}$ and $C_{b,e}$, as well as the mixed inlet concentration $C^{o}_{a,i}$, are not specified a priori. Mathematically, two more relations are needed for determination of these values. For this purpose, two mass balances for solutes at the inlet of phase *a* and through the whole module are readily obtained, respectively, as

$$C_{a,i} + RC'_{a,e} = (1+R)C^{\circ}_{a,i} \tag{33}$$

$$C_{b,e} = C_{b,i} + (\frac{Q_a}{Q_b})(C_{a,i} - C_{a,e}) \tag{34}$$

By solving Eqs.(27), (28) and (33) simultaneously,one has

$$C^{\circ}_{a,i} = [\frac{R(BE-AF)}{B+BR-FR}]C_{b,e} + (\frac{B}{B+BR-FR})C_{a,i} \tag{35}$$

$$C_{a,e} = [\frac{ER-A(1+R)}{B+BR-FR}]C_{b,e} + (\frac{1}{B+BR-FR})C_{a,i} \tag{36}$$

Substituting Eq.(34) into Eq.(36), we obtain the outlet concentration from phase a

$$C_{a,e} = \{\frac{Q_a[ER-A(1+R)]+Q_b}{Q_b(B+BR-FR)+Q_a[ER-A(1+R)]}\}C_{a,i}$$

$$+\{\frac{Q_b[ER-A(1+R)]}{Q_b(B+BR-FR)+Q_a[ER-A(1+R)]}\}C_{b,i} \tag{37}$$

Substitution of Eq.(37) into Eq.(34) gives the expression for calculation of the outlet concentration from phase b, $C_{b,e}$.

乙、 *Countercurrent-flow operation with concurrent-flow reflux*

Figure 2, shows a schematic diagram of the rectangular system of countercurrent-flow membrane extraction with concurrent-flow reflux. Referring to Fig. 2, the mass balance over the right-hand section of the membrane extractor operated, with reflux ratio *R*, is

$$Q_b(C_b - C_{b,i}) = (1+R)Q_a C_{a,1} - RQ_a C_{a,2} - Q_a C_{a,e} \tag{38}$$

or

$$C_b = C_{b,i} + (\frac{Q_a}{Q_b})\left[(1+R)\ Q_a C_{a,1} - RQ_a C_{a,2} - C_{a,e}\ \right] \tag{39}$$

Considering the mass transfer on subchannels a_1 and a_2 over the length *dx*

$$-(1+R)Q_a dC_{a,1} = K_1 \Delta w(H_{ac}C_{a,1} - H_{bc}C_b)dx \tag{40}$$

$$RQ_a dC_{a,2} = K_2(1-\Delta)\mathrm{w}(H_{ac}C_{a,2} - H_{bc}C_b)dx \tag{41}$$

Substituting the value of C_b from Eq. (39) into Eqs. (40) and (41), one obtains

$$\frac{dC_{a,1}}{dx} + \zeta' C_{a,1} - \zeta^0 C_{a,2} = \varsigma C_{b,i} - \varsigma^0 C_{a,e} \tag{42}$$

$$\frac{dC_{a,2}}{dx} + \varpi' C_{a,2} - \varpi^\circ C_{a,1} = \xi C_{b,i} - \xi^\circ C_{a,e} \tag{43}$$

Ca,e can be solved from Eqs.(42) and (43) by following the same mathematical procedure performed in section 2.1. with the use of the additional mass balances, Eqs.(33) and (34), as well as the appropriate boundary conditions, Eqs.(16), (25) and (26).

The result is

$$C_{a,e} = [\frac{E'R - A'(1+R)}{B' + B'R - F'R}]C_{b,i} + (\frac{1}{B' + B'R - F'R})C_{a,i} \tag{44}$$

where

$$A' = \frac{(n'\lambda_b' + \varsigma)e^{-\lambda_a' L} - (n'\lambda_a' + \varsigma)e^{-\lambda_b' L}}{(\lambda_a' - \lambda_b')} + n' \tag{45}$$

$$B' = \frac{(m'\lambda_b' + \varsigma^\circ - \lambda_b' - \zeta' - \zeta^\circ)e^{-\lambda_a' L}}{(\lambda_a' - \lambda_b')} - \frac{(m'\lambda_a' + \varsigma^\circ - \lambda_a' - \zeta' - \zeta^\circ)e^{-\lambda_b' L}}{(\lambda_a' - \lambda_b')} + m' \tag{46}$$

$$E' = \frac{1}{\zeta^\circ}[\frac{(\lambda_a' + \zeta')(n'\lambda_b' + \varsigma)e^{-\lambda_a' L}}{(\lambda_b' - \lambda_a')} - \frac{(\lambda_b' + \zeta')(n'\lambda_a' + \varsigma)e^{-\lambda_b' L}}{(\lambda_b' - \lambda_a')} + (\varsigma - \zeta' n')] \tag{47}$$

$$F' = \frac{1}{\zeta^\circ}[\frac{(\lambda_a' + \zeta')(m'\lambda_b' + \varsigma^\circ - \lambda_b' - \zeta' - \zeta^\circ)e^{-\lambda_a' L}}{(\lambda_b' - \lambda_a')}$$

$$- \frac{(\lambda_b' + \zeta')(m'\lambda_a' + \varsigma^\circ - \lambda_a' - \zeta' - \zeta^\circ)e^{-\lambda_b' L}}{(\lambda_b' - \lambda_a')} + (\varsigma^\circ - \zeta' m')] \tag{48}$$

$$\zeta' = K_1 \Delta w[\frac{H_{ac}}{(1+R)Q_a} - \frac{H_{bc}}{Q_b}] \tag{49}$$

$$\varpi' = -K_2(1-\Delta)w(\frac{H_{ac}}{RQ_a} + \frac{H_{bc}}{Q_b}) \tag{50}$$

$$\lambda_a' = \frac{-(\zeta' + \varpi') + \sqrt{(\zeta' - \varpi')^2 + 4\zeta^\circ \varpi^\circ}}{2} \tag{51}$$

$$\lambda_b' = \frac{-(\zeta' + \varpi') - \sqrt{(\zeta' - \varpi')^2 + 4\zeta^\circ \varpi^\circ}}{2} \tag{52}$$

$$n' = \frac{\varpi'\varsigma - \zeta^\circ \xi}{\zeta'\varpi' - \zeta^\circ \varpi^\circ} \tag{53}$$

$$m' = \frac{-\varpi'\varsigma^\circ - \zeta^\circ \xi^\circ}{\zeta'\varpi' - \zeta^\circ \varpi^\circ} \tag{54}$$

2. 3. Mass-transfer rate

Once the outlet concentrations, $C_{a,e}$ and $C_{b,e}$, obtained from Eqs.(37) and (34) and from Eqs.(46) and (34), respectively, for councurrent-flow and countercurrent-flow operations, the total mass-transfer rates will be determined by Eq. (55).

$$W = Q_a(C_{a,i} - C_{a,e}) = Q_b(C_{b,e} - C_{b,i}) \tag{55}$$

3. Numerical Example

For the purpose of illustration, let us employ the experimental data of previous work[13]. Experiments were carried out with the use of a membrane sheet (l=w=0.165m) made of microporous polypropylene(Gelman Sciences, average pore size=0.2 μm, porosity=70% and thickness=178 μm) as a permeable barrier to extract acetic acid(reagent ACS grade, Fisher) from aqueous solution by methyl isobutyl ketone (MIBK, regent grade, Fisher). The membrane sheet was inserted in parallel between two parallel plates of stainless steel, with same distance from them to divide the conduit into two channels(channels a and b, or phases a and b) of same height ($h = 1.9\times10^{-3}$ m). Since microporous polypropylene is hydropholic membranes, the organic solution (solute: acetic; solvent: MIBK) wets the membrane, and thus $H_{bc} = 1$ and $H_{ac} = 0.524$ at $25\,^{o}C$ [15].

The following correlation equations for estimating the average values of overall mass-transfer coefficient applicable to such small velocity ranges (Q_a=0.188~0.847 cm^3/s, Q_b=0.25cm^3/s) were obtained [13] as :

For $C_{a,i} = 5\times10^{-4} mole/cm^3$:

$$K_i \times 10^4 (cm/s) = 3.865 + 1.484 v_{a,i}(cm/s)$$ (concurrent flow; i=1 for Section 2.1. and i=2 for Section 2.2.) (56)

$$K_i \times 10^4 (cm/s) = 5.012 + 0.718 v_{a,i}(cm/s)$$ (countercurrent flow; i=1 for Section 2.2. and i=2 for Section 2.1.) (57)

For $C_{a,i} = 2.02\times10^{-3}$ $mole/cm^3$:

$$K_i \times 10^4 (cm/s) = 2.152 + 0.846 v_{a,i}(cm/s)$$ (concurrent flow; i=1 for Section 2.1. and i=2 for Section 2.2.) (58)

$$K_i \times 10^4 (cm/s) = 3.177 + 0.733 v_{a,i}(cm/s)$$ (countercurrent flow; i=1 for Section 2.2. and i=2 for Section 2.1.) (59)

in which the fluid velocities, $v_{a,1}$ and $v_{a,2}$ (cm/s), in phase a is related with the reflux ratio R as

$$v_{a,1} = \frac{Q_a(1+R)}{h\Delta w}$$ (60)

$$v_{a,2} = \frac{Q_a R}{h(1-\Delta)w}$$ (61)

4. Results and discussion

4.1. Effect of Δ on performance

It is seen in Fig.3 that for the device of concurrent-flow operation with countercurrent-flow reflux, mass-transfer rate increases when the width ratio (Δ) of concurrent-flow channel (subchannel a_1) to countercurrent-flow channel (subchannel a_2) decrease. On the other hand, Fig. 4 shows that for the device of countercurrent-flow operation with concurrent-flow reflux, mass-transfer rate increases with the width ratio(Δ) of countercurrent-flow channel (subchannel a_1) to concurrent-flow channel (subchannel a_2). These are because that for mass transfer, the countercurrent-flow effect is more effective than the concurrent-flow effect, and that larger part of mass-transfer area for countercurrent-flow channel, as well as smaller part of mass-transfer area for concurrent-flow channel, is beneficial to total mass-transfer rate. Further, the modules of higher inlet concentration overcomes the modules of lower inlet concentration, as comparing Fig. (3a) with Fig. (3b), as well as Fig. 4(a) with Fig. 4(b).

It is better to illustrate the improvement of performance *I* based on that obtained with the recycle barrier located at the centerline (Δ=0.5) of the raffinate phase

$$I = \frac{W - W_{\Delta=0.5}}{W_{\Delta=0.5}} \tag{62}$$

The results are listed in Tables 1 and 2 for two types of operation. It is seen in these tables that *I* obtained in the second type by increasing the mass-transfer area for countercurrent-flow operation (Δ>0.5), as shown in Fig. 2(a), overcomes that obtained in the first type by increasing the mass-transfer area for countercurrent-flow reflux (Δ<0.5), as shown in Fig. 1(a). This is because that the flow rates for countercurrent-flow operation, $(1+R)Q_a$, is larger than that for countercurrent-flow reflux, RQ_a, leading to further improved performance, especially for small Q_a and R.

4.2. Effect of Δ on reduction of R

Figures 5 and 6 illustrate the comparision of the performance obtained for R=1 and Δdiffering from 0.5 with that obtained for Δ=0.5 and R larger than unity, under low flow-rate operations in raffinate phase. It is seen in these figures that with the recycle-barrier location moving gradually from the centerline ($\Delta \rightarrow 0$ for concurrent-flow operation, and $\Delta \rightarrow 1$ for countercurrent-flow operation, of the systems described in Section 2.1. and Section 2.2., respectively), the number of reflux ratio R reguired may be gradually reducing for obtaining the same performance. As we can see in Fig. 5(b) that the mass-transfer rate W for Δ=0.1 and R=1 is larger than that for Δ=0.5 and R=2 while in Fig.6(b), W for Δ=0.9 and R=1 is larger than that for Δ=0.5 and R=3.

Some numerical values of predicting result for W are listed in Tables 1 and 2, which give the same results described above.

5. Conclusion

The performance of membrane extraction through rectangular mass exchangers with internal reflux has been analyzed under cocurrent-flow and countercurrent-flow operations. The ordinary differential equations for solute concentration distributions in the raffinate and extract phases were derived based on mass balances with the assumptions of uniform concentrations and velocities over cross-sections of flow channels. The outlet concentration were solved simultaneously from the governing equations with the use of appropriate boundary conditions. Once the outlet concentrations were obtained, the overall mass-transfer rates *W* for two types of flow

were predicted. The results are plotted in Figs 3-6 and listed in Tables 1 and 2. It is found that W increases with Q_a, $C_{a,i}$ and R, as well as with Δ of values approaching zero for concurrent-flow operation and approaching unity for countercurrent-flow operation. It is also noted that the order of mass transfer rate in two types of mass exchanger is: *countercurrent-flow operation with concurrent-flow reflux > concurrent-flow operation with countercurrent-flow reflux.*

The effect of recycle-barrier location on performance was also further investigated. It was found that larger part of mass-transfer area for countercurrent-flow channel as well as smaller part of mass-transfer area for concurrent-flow channel, is benifical to total mass-transfer rate, and that with the recycle-barrier location moving gradually from the centerline to create larger mass-transfer area for countercurrent-flow channel, the reflux ratio can be reduced for achieving the same performance.

7. List of symbols

A, B, E, F	Constant defined by Eqs. (29)-(32)
A', B', C', F'	Constant defined by Eqs. (45)-(48)
C_a, C_b	Bulk solute concentrations in raffinate phase (phase a), and in extract phase (phase b) ($mole/cm^3$)
$C_{a,e}, C_{b,e}$	Outlet solute concentrations in phase a. and in phase b ($mole/cm^3$)
$C'_{a,e}$	Outlet concentration in subchannel a_2 ($mole/cm^3$)

$C_{a,i}, C_{b,i}$	Inlet solute concentration in phase a, in phase b ($mole/cm^3$)
$C^o_{a,i}$	Mixed inlet concentration in phase a ($mole/cm^3$)
C_{a1}, C_{a2}	Bulk solute concentrations in subchannel a_1, in subchannel a_2 of phase a ($mole/cm^3$)
$n,\ n'$	Constant defined by Eq. (21) and Eq.(53), respectively
$m,\ m'$	Constant defined by Eq. (22) and Eq.(54), respectively
H_{ij}	Distribution coefficient between phase i and phase j
h	Half height of parallel channel, or distance between flat plate and membrane sheet (cm)
K_i	Average overall mass-transfer coefficient (cm/s), i=1 and 2(cm/s)
L	The length of membrane sheet (cm)
Q_a, Q_b	Inlet volume rates in phase a, in phase b (cm^3/s)
R	Reflux ratio, reverse volume rate RQ_a divided by inlet volume rate Q_a
S	Overall mass-transfer area of a flat-plate membrane module Lw, (cm^2)
$v_{a,1}, v_{a,2}$	Fluid velocity in subchannel a_1, in subchannel a_2 (cm/s)
v_b	Fluid velocity in phase b (cm/s)
w	Width of membrane sheet (cm)
x	Axis along the flow direction
I	Improvement in performance defined by Eq. (62)

6. 1. Greek letters

α	Constant defined by Eq. (23)
β	Constant defined by Eq. (24)
Δ	Width fraction of subchannel a_1, $\Delta w/w$
ζ,ζ^0,ζ'	Constant defined by Eqs. (8), (9) and (49), respectively
ς,ς^0	Constant defined by Eqs. (10) and (11), respectively
ϖ,ϖ^0,ϖ'	Constant defined by Eqs. (12), (13) and (50), respectively
ξ,ξ^0	Constant defined by Eqs. (14) and (15), respectively
λ_a,λ_b	Constant defined by Eqs. (19) and (20), respectively
λ_a',λ_b'	Constant defined by Eqs. (51) and (52), respectively

7. Acknowledgements

We wish to express our thanks to the National Science Council of R. O. C. for financial aid under Grand No. NSC-91-2214-E-032-001 and Grand No. NSC-92-2214-E-032-001.

8. References

[1] T.C. Lo, M.H.I. Baird, Liquid-Liquid extraction, in: M. Grayson

(Ed.), Kirktothmer Encyclopedia of Chemical Technology, Vol. 9, 3rd Edition, Wiley, New York, 1980.

[2] S.W. Tsai, H.M. Yeh, A study of the separation efficiency in horizontal thermal diffusion columns with external refluxes, Can. J. Chem. Eng. 63 (1985) 406.

[3] H.M. Yeh, S.W. Tsai, C.S. Lin, A study of the separation efficiency in thermal diffusion column with a vertical permeable barrier, AIChE J. 32 (1986) 971.

[4] H.M. Yeh, T.W. Cheng, S.W. Tsai, A study of the gratez problem in concentric-tube continuous-contact countercurrent separation processes with recycles at both ends, Sep. Sci. Technol. 21 (1986) 403.

[5] H.M. Yeh, S.W. Tsai, C.L. Chiang, Recycle effects on heat and mass transfer through a parallel-plate channel, AIChE J. 33 (1987) 1743.

[6] C.D. Ho, H.M. Yeh, W.S. Sheu, The analytical studies of heat and mass transfer through a parallel-plate channel with recycle, Int. J. Heat Mass Transfer 41 (1988) 2589.

[7] J. Korpijarvi, P. Oinas, J. Reunanen, Hydrodynamics and mass transfer in airlift reactor, Chem. Eng. Sci. 54 (1998) 2255.

[8] E. Santacesaria, M. Di Serio, P. Iengo, Mass transfer and kinetics in ethoxylation spray tower loop reactors, Chem. Eng. Sci. 54 (1999) 1499.

[9] E. Garcia-Calvo, A. Rodriguez, A. Prados, J. Klein, Fluid dynamic model for three-phase airlift reactors, Chem. Eng. Sci. 54 (1998) 2359.

[10] M. Stenas, M. Clark, V. Lazarova, Holdup and liquid circulation velocity in a rectangular air-lift bioreactor, Ind. Eng. Chem. Res. 38 (1999) 944.

[11] S. Goto, P.D. Gaspillo, Effect of static mixer on mass transfer in draft tube bubble column and in external loop cilomn, Chem. Eng. Sci. 47 (1992) 3533.

[12] K.I. Kikuchi, H. Takahashi, Y. Takeda, F. Sugawara, Hydrodynamic behavior of single particles in a draft-tube bubble column, Can. J. Chem. Eng. 77 (1999) 573.

[13] H.M. Yeh, Y.Y. Peng, Y.K. Chen, Solvent extraction through a double-pass parallel-plate membrane channel with recycle, J. Membr. Sci. 163 (1999) 177.

[14] H.M. Yeh, C.H. Chen, Recycle effects on solvent extraction through concurrent-flow parallel-plate membrane modules, J. Membr. Sci. 190(2001) 35.

[15] H.M. Yeh, C.M. Huang, Solvent extraction in multipass parallel-flow mass exchangers of microporous hollow-fiber modules, J. Membr. Sci. 103 (1995) 135.

Figure Legends

Fig. 1. Parallel-plate membrane extractor with concurrent-flow operation and countercurrent-flow reflux.

Fig. 2. Parallel-plate membrane extractor with countercurrent-flow operation and concurrent-flow reflux.

Fig. 3. Mass-transfer rate obtained in the device of concurrent-flow operation with countercurrent-flow reflux.

Fig. 4. Mass-transfer rate obtained in the device of countercurrent-flow operation with concurrent-flow reflux.

Fig. 5. Comparison of W obtained under cocurrent-flow operation for R=1 and Δ=0.1~0.5 with that for Δ=0.5 and R=2~3.

Fig. 6. Comparison of W obtained under countercurrent-flow operation for R=1 and Δ=0.5~0.9 with that for Δ=0.5 and R=2~3.

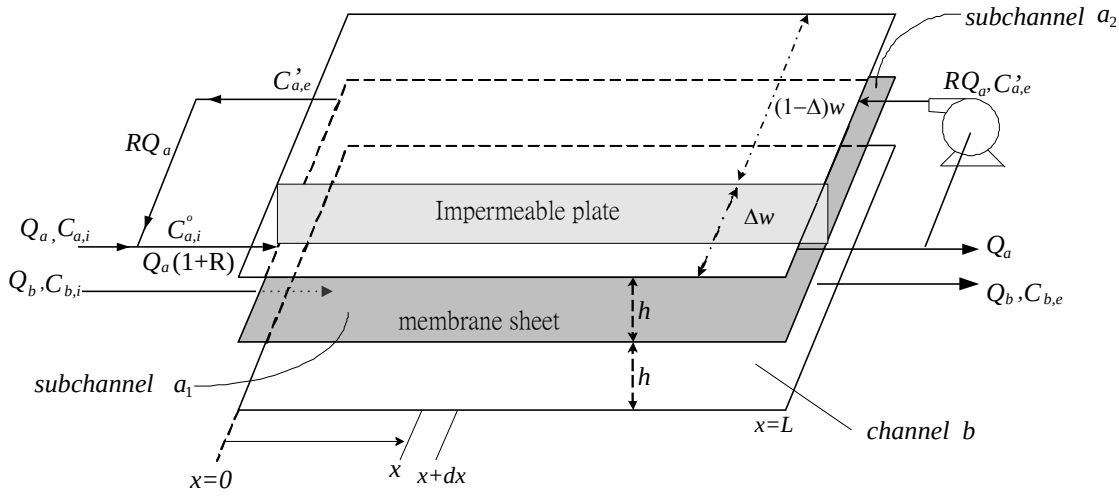

(a) Schematic diagram

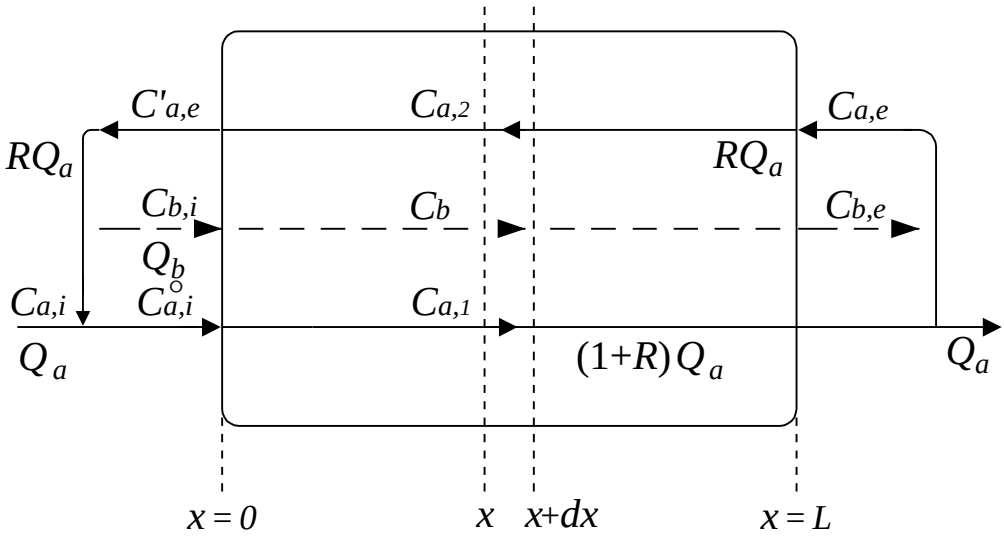

(b) Flow chart

Fig. 1

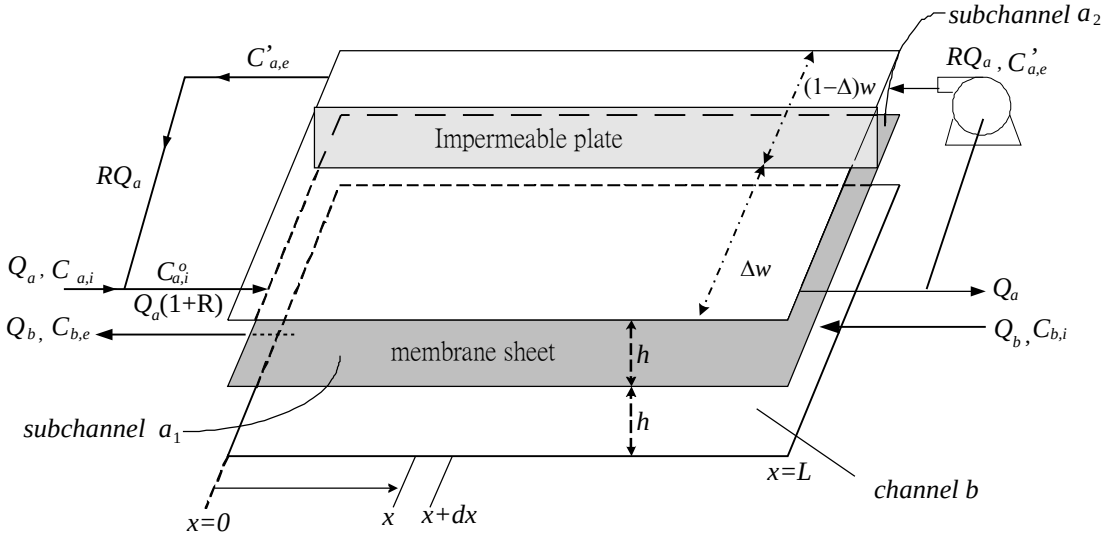

(a) Schematic diagram

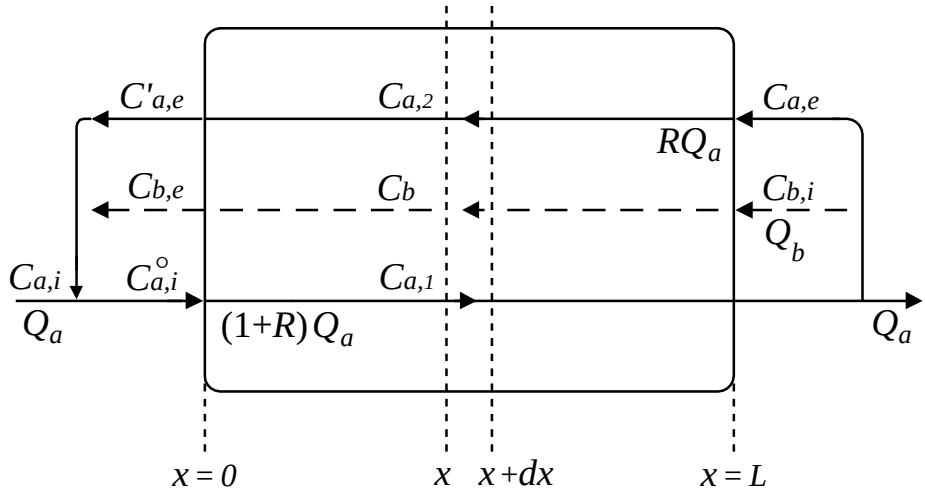

(b) Flow chart

Fig. 2

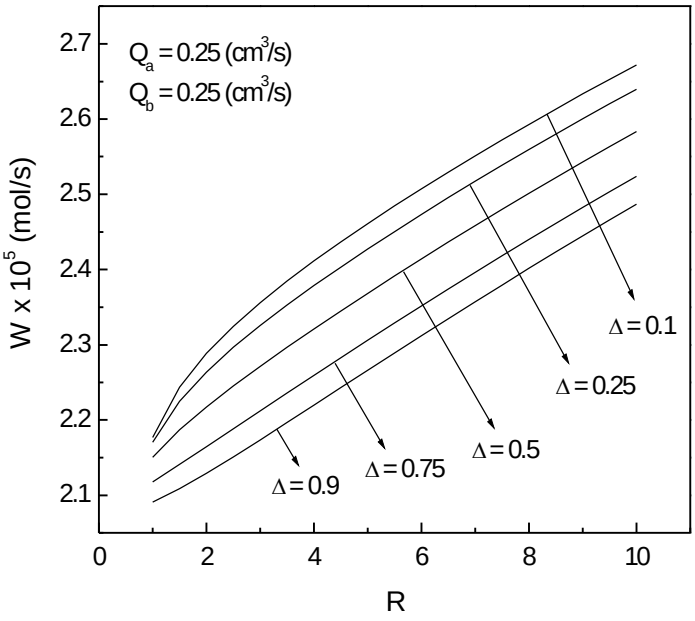

(a) $C_{a,i} = 0.5 \times 10^{-3} mole / cm^3$

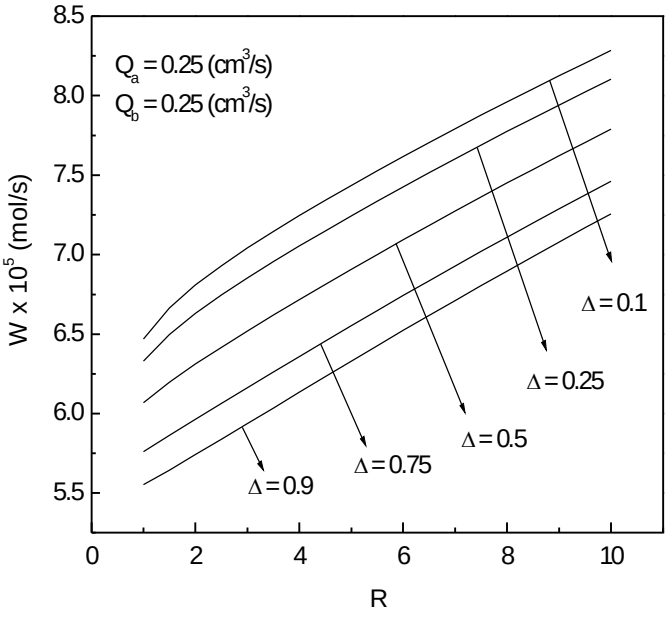

(b) $C_{a,i} = 2.0 \times 10^{-3} mole / cm^3$

Fig. 3

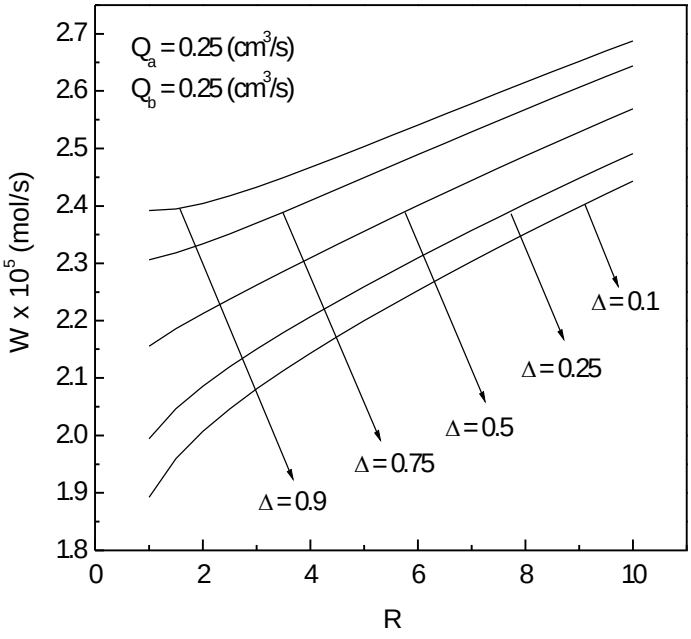

(a) $C_{a,i} = 0.5 \times 10^{-3} mole/cm^3$

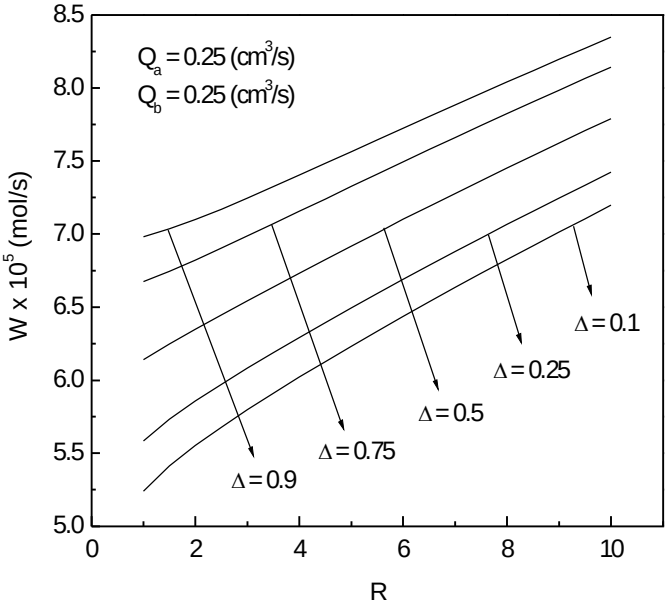

(b) $C_{a,i} = 2.0 \times 10^{-3} mole/cm^3$

Fig. 4

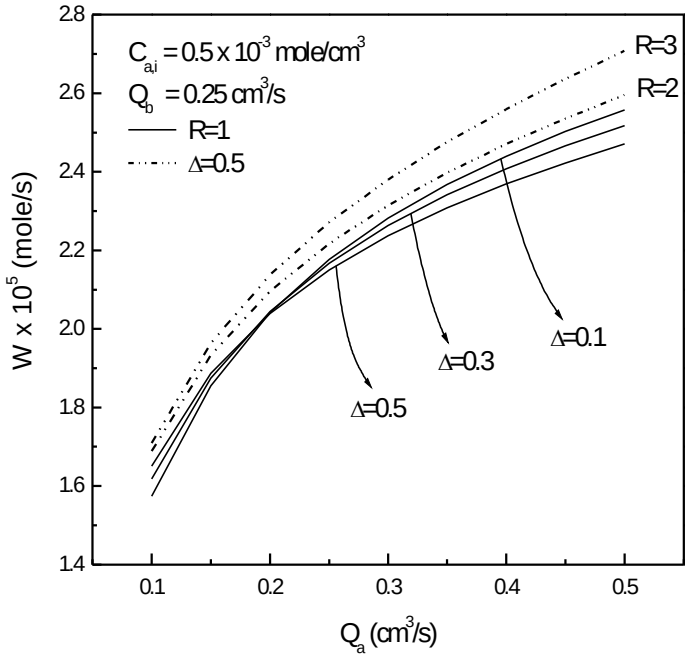

(a) $C_{a,i} = 0.5 \times 10^{-3} mole/cm^3$

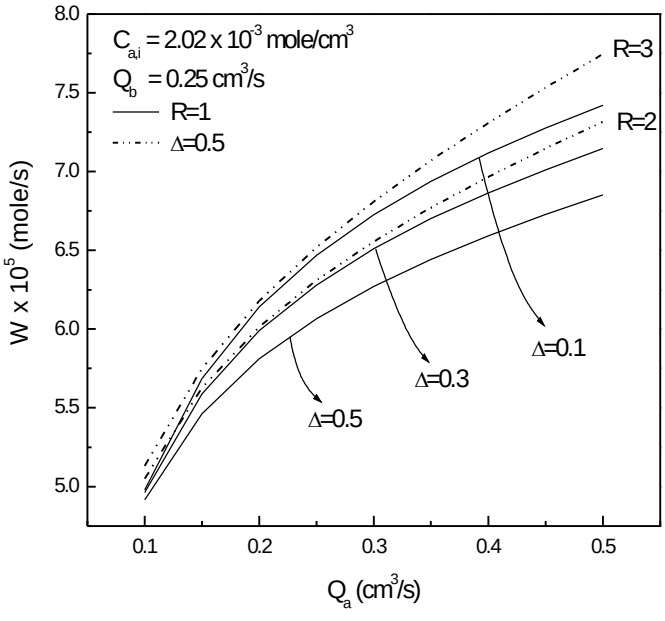

(b) $C_{a,i} = 2.0 \times 10^{-3} mole/cm^3$

Fig. 5

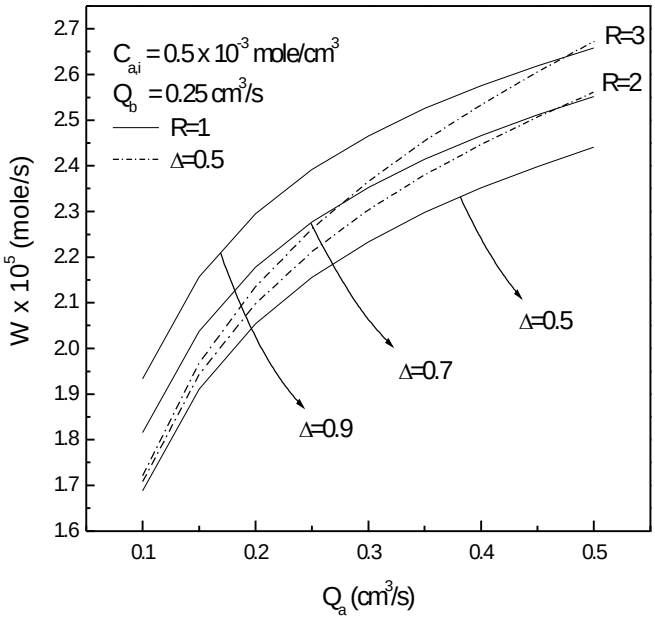

(a) $C_{a,i} = 0.5 \times 10^{-3} mole/cm^3$

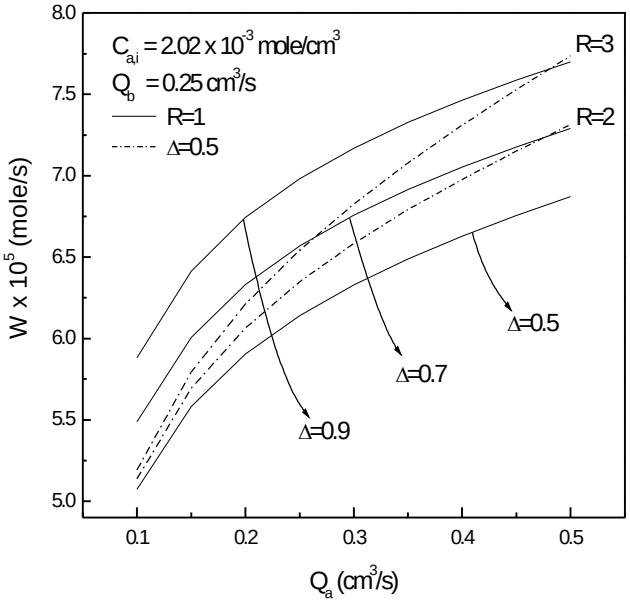

(b) $C_{a,i} = 2.0 \times 10^{-3} mole/cm^3$

Fig. 6

Table 1a

Predicting results of concurrent-flow operation with countercurrent-flow reflux :

$C_{a,i} = 0.5 \times 10^{-3} mole/cm^3$, $Q_b = 0.25 cm^3/s$ and $C_{b,i} = 0$

Q_a (cm^3/s)	R	$W \times 10^{-5}$ (mole/s)	I (%)			
		Δ=0.5	Δ=0.1	Δ=0.25	Δ=0.75	Δ=0.9
0.2	1	2.0394	0.10	0.25	-0.93	-1.86
0.2	5	2.2125	3.72	2.38	-2.55	-4.18
0.2	9	2.3459	3.58	2.27	-2.41	-3.92
0.4	1	2.3693	2.98	1.98	-2.41	-4.09
0.4	5	2.7238	3.91	2.48	-2.61	-4.24
0.4	9	3.0123	3.19	2.02	-2.11	-3.42
0.6	1	2.5560	3.86	2.50	-2.82	-4.69
0.6	5	3.0838	3.57	2.26	-2.36	-3.82
0.6	9	3.4986	2.63	1.66	-1.72	-2.79
0.8	1	2.6982	4.17	2.68	-2.94	-4.84
0.8	5	3.3839	3.17	2.00	-2.08	-3.37
0.8	9	3.8967	2.15	1.36	-1.41	-2.28

Table 1b

Predicting results of concurrent-flow operation with countercurrent-flow reflux :

$C_{a,i} = 2.02 \times 10^{-3} mole/cm^3$, $Q_b = 0.25 cm^3/s$ and $C_{b,i} = 0$

Q_a (cm^3/s)	R	$W \times 10^{-5}$ (mole/s)	I (%)			
		Δ=0.5	Δ=0.1	Δ=0.25	Δ=0.75	Δ=0.9
0.2	1	5.8112	5.66	3.76	-4.57	-7.76
0.2	5	6.4799	7.64	4.86	-5.18	-8.45
0.2	9	7.0338	6.83	4.34	-4.58	-7.45
0.4	1	6.5919	7.97	5.12	-5.66	-9.34
0.4	5	7.9527	7.19	4.55	-4.76	-7.73
0.4	9	9.1207	5.69	3.60	-3.75	-6.07
0.6	1	7.0786	8.44	5.39	-5.80	-9.49
0.6	5	9.1091	6.35	4.01	-4.17	-6.75
0.6	9	10.8066	4.62	2.92	-3.02	-4.89
0.8	1	7.4781	8.44	5.37	-5.71	-9.30
0.8	5	10.1365	5.57	3.52	-3.65	-5.90
0.8	9	12.2793	3.79	2.40	-2.48	-4.00

Table 2a

Predicting results of countercurrent -flow operation with concurrent -flow reflux :

$C_{a,i} = 0.5 \times 10^{-3} mole/cm^3$, $Q_b = 0.25 cm^3/s$ and $C_{b,i} = 0$

Q_a (cm^3/s)	R	$W \times 10^{-5}$ (mole/s)	I (%)			
		Δ=0.5	Δ=0.1	Δ=0.25	Δ=0.75	Δ=0.9
0.2	1	2.0534	-13.18	-8.06	7.51	11.77
0.2	5	2.2054	-6.95	-4.30	4.14	6.56
0.2	9	2.3360	-5.48	-3.38	3.26	5.16
0.4	1	2.3514	-10.42	-6.41	6.06	9.53
0.4	5	2.6969	-5.80	-3.59	3.47	5.50
0.4	9	2.9867	-4.28	-2.65	2.56	4.06
0.6	1	2.5137	-9.16	-5.64	5.36	8.46
0.6	5	3.0413	-4.93	-3.05	2.95	4.68
0.6	9	3.4620	-3.39	-2.10	2.03	3.22
0.8	1	2.6347	-8.34	-5.14	4.91	7.75
0.8	5	3.3290	-4.24	-2.62	2.54	4.03
0.8	9	3.8524	-2.73	-1.69	1.64	2.60

Table 2b

Predicting results of countercurrent -flow operation with concurrent -flow reflux :

$C_{a,i} = 2.02 \times 10^{-3} mole/cm^3$, $Q_b = 0.25 cm^3/s$ and $C_{b,i} = 0$

Q_a (cm^3/s)	R	$W \times 10^{-5}$ (mole/s)	I (%)			
		Δ=0.5	Δ=0.1	Δ=0.25	Δ=0.75	Δ=0.9
0.2	1	5.9052	-15.34	-9.45	9.01	14.21
0.2	5	6.4975	-10.31	-6.37	6.13	9.69
0.2	9	7.0403	-8.51	-5.25	5.04	7.97
0.4	1	6.6284	-13.40	-8.28	7.97	12.61
0.4	5	7.9469	-8.73	-5.40	5.23	8.29
0.4	9	9.1101	-6.63	-4.10	3.97	6.29
0.6	1	7.0833	-12.29	-7.60	7.34	11.63
0.6	5	9.0875	-7.45	-4.61	4.47	7.09
0.6	9	10.7845	-5.27	-3.26	3.16	5.02
0.8	1	7.4596	-11.46	-7.09	6.86	10.87
0.8	5	10.1025	-6.43	-3.98	3.87	6.13
0.8	9	12.2485	-4.29	-2.66	2.58	4.09